Pre-Steady State Kinetic Analysis of an Enzymatic Reaction Monitored by Time-Resolved Electrospray Ionization Mass Spectrometry†

David L. Zechel, Lars Konermann, Stephen G. Withers,* and D. J. Douglas

Department of Chemistry, University of British Columbia, 2036 Main Mall, Vancouver, British Columbia V6T 1Z1, Canada

Received February 24, 1998; Revised Manuscript Received April 2, 1998

ABSTRACT: For the first time, the new technique of time-resolved electrospray ionization mass spectrometry (ESI-MS) has been used to accurately measure the pre-steady state kinetics of an enzymatic reaction by monitoring a transient enzyme intermediate. The enzyme used to illustrate this approach, *Bacillus circulans* xylanase, is a retaining glycosidase that hydrolyzes xylan or β-xylobiosides through a double-displacement mechanism involving a covalent xylobiosyl−enzyme intermediate. A low steady state level of this intermediate formed during the hydrolysis of 2,5-dinitrophenyl β-D-xylobioside was detected by time-resolved ESI-MS. The low concentration of this intermediate and its rate of formation did not permit pre-steady state kinetic analysis. By contrast, the covalent intermediate accumulates fully when the Tyr80Phe mutant hydrolyzes the same substrate. Using time-resolved ESI-MS, the pre-steady state kinetic parameters for the formation of the covalent intermediate in the mutant xylanase have been determined. The kinetic data are in agreement with those determined by monitoring the release of 2,5-dinitrophenol with stopped-flow UV−vis spectroscopy. This demonstrates that time-resolved ESI-MS can be used to accurately monitor the pre-steady state kinetics of enzymatic reactions, with the advantage of identifying transient enzyme intermediates by their mass.

Electrospray ionization mass spectrometry (ESI-MS)[1] plays a well-established role in investigations on the primary structure of proteins and other biomolecules (*1*, *2*). This technique is also becoming increasingly important in different fields such as the study of noncovalent protein−ligand and protein−protein interactions (*3*), protein folding (*4*−*7*), and the structures of gas phase proteins (*8*−*10*). During ESI, intact protein ions in the gas phase are generated from proteins in solution. In the commonly used positive-ion mode of operation, these ions are multiply charged due to the attachment of protons (*3*, *11*, *12*). The new method of "time-resolved" ESI-MS, which couples a continuous-flow mixing capillary directly to an ESI source, allows the rates of (bio)chemical reactions to be monitored with a mass spectrometer. At the current state of development, it can be used to measure reaction kinetics on a time scale of tens of milliseconds (*13*). The first successful application of time-resolved ESI-MS on a subsecond time scale involved the study of protein folding kinetics (*13*, *14*). Different protein conformations in solution were identified by the different charge state distributions they generate during ESI. It was demonstrated that this technique is especially useful in studying the kinetics of folding reactions that are coupled to the loss or binding of a ligand. Protein states with and without ligand can be easily separated by their different masses if the ligand−protein interactions are not disrupted during ESI.

Recently, it was proposed that time-resolved ESI-MS could become a powerful tool for monitoring the kinetics of enzymatic reactions (*15*). Potentially, ESI-MS will allow the simultaneous detection of substrates, intermediates, and products of enzymatic reactions, as well as the detection of covalent or noncovalent enzyme−substrate complexes. The use of ESI-MS could obviate the need for chromophoric substrates and coupled assays that are currently required for monitoring the kinetics of most enzymatic reactions. Indeed, the detection of enzymes complexed with inhibitors (*16*), substrates (*17*), and products (*17*) by ESI-MS (*17*) has been demonstrated previously. Likewise, covalent enzyme intermediates have been detected in serine proteases (*18*), elastase (*19*), β-lactamase (*20*−*22*), and several glycosidases (*23*, *24*). Lee et al. (*25*) used a continuous sample introduction system to monitor the steady state kinetics of lactase. More recently, a pulsed-flow device coupled to ESI-MS, operating on a 30 ms time scale, was used successfully to detect a highly unstable tetrahedral intermediate in the reaction catalyzed by 5-enolpyruvoylshikimate-3-phosphate synthase (*26*), but no kinetic parameters were determined. However, a stopped-flow device coupled to ESI-MS, capable of detection on a 25 ms time scale, was used to monitor the Britton reverse transport kinetics of carbonic anhydrase (*27*).

This study is the first in which time-resolved ESI-MS has been used to determine the pre-steady state kinetics of an enzymatic reaction by direct observation of a transient

† This work was supported by the Natural Sciences and Engineering Research Council of Canada (NSERC) and by an NSERC-SCIEX Industrial Chair.

* To whom correspondence should be addressed. Phone: (604) 822-3402. Fax: (604) 822-2847. E-mail: withers@chem.ubc.ca.

[1] Abbreviations: 8^+, 9^+, etc., charge states of protein ions in the gas phase ([protein + $8H^+$]$^{8+}$, [protein + $9H^+$]$^{9+}$, etc.); BCX, *Bacillus circulans* xylanase; E−X_2, covalent xylobiosyl−enzyme intermediate; 2,5-$DNPX_2$, 2,5-dinitrophenyl β-xylobioside; 2,5-DNP, 2,5-dinitrophenol; ESI, electrospray ionization; MS, mass spectrometry; MS−MS, tandem mass spectrometry; *m*/*z*, mass-to-charge ratio.

S0006-2960(98)00445-0 CCC: $15.00
Published on Web 05/08/1998

Scheme 1: Mechanism for the Hydrolysis of 2,5-$DNPX_2$ by *B. circulans* Xylanase (BCX)

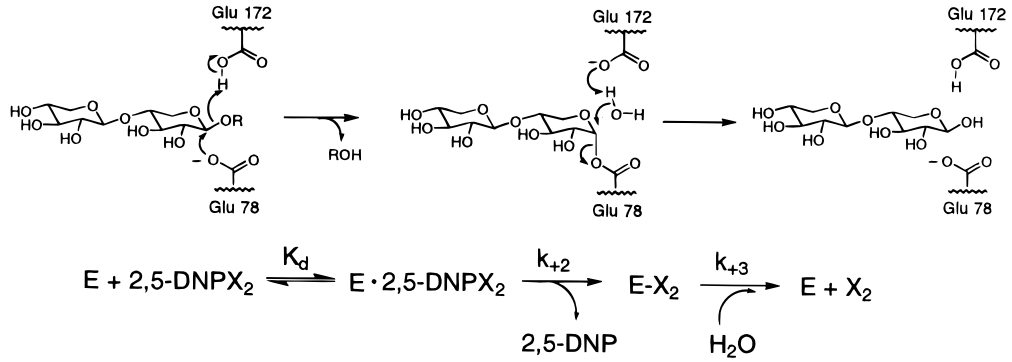

enzyme intermediate. A mutant of the extensively characterized *Bacillus circulans* xylanase (BCX, EC 3.2.1.8) was chosen as a model enzyme system. This is a small family 11 (*28*) glycosidase that cleaves the β-1,4 glycosidic bonds of xylan to release xylobiose. Hydrolysis occurs with retention of anomeric configuration (*29*), necessarily implying the involvement of a covalent xylobiosyl−enzyme intermediate ($E-X_2$) as part of a classical double-displacement mechanism (Scheme 1) (*30*, *31*). This mechanism generally involves two carboxyl residues that are diametrically opposed in the glycosidase active site. The three-dimensional structure of BCX has been solved by X-ray crystallography (*32*) and NMR spectroscopy (*33*); the former, complemented by mutagenesis, led to the initial assignment of Glu78 as the nucleophile and Glu172 as the general acid−base catalyst. This assignment was confirmed by trapping the covalent intermediate with the mechanism-based inactivator 2,4-dinitrophenyl 2-deoxy-2-fluoro-β-xylobioside (*34*). Analysis of the proteolytically digested enzyme by ESI-MS−MS in the neutral-loss mode (*35*) identified Glu78 as the nucleophile. This detailed mapping of the active site, as well as the small size of the enzyme, has allowed the study of fundamental aspects of the retaining glycosidase mechanism. For example, the catalytic consequences of modifying the distance between these two carboxyl residues were probed by mutagenesis (*36*, *37*), and the phenomenon of "pK_a cycling" of Glu172 during catalysis was monitored by ^{13}C NMR (*38*).

Pre-steady state analysis has been applied widely to the study of transient intermediates in enzymic reactions (*39*−*42*), including the covalent intermediates formed by retaining glycosidases. Stopped-flow UV−vis spectroscopy was used to determine the glycosylation and deglycosylation rate constants for *Cellulomonas fimi* β-1,4-glycanase (*43*, *44*) and *Agrobacterium* sp. β-glucosidase (*45*−*47*) using substrates that were hydrolyzed with rate-limiting deglycosylation. Likewise, the pre-steady state "bursts" of phenolate observed for the hydrolysis of reactive aryl-β-galactosides by *Escherichia coli (lac Z)* β-galactosidase provided early evidence of a glycosyl−enzyme intermediate (*48*−*50*). Wild type BCX has not been amenable to pre-steady state kinetic analysis by stopped-flow UV−vis spectroscopy due to the fact that the glycosylation step is rate-limiting with all known synthetic substrates (*37*). However, as shown in this study, the deglycosylation step is rate-limiting for the Y80F mutant with the substrate 2,5-$DNPX_2$, leading to accumulation of $E-X_2$ at a rate that can be monitored in the pre-steady state phase by time-resolved ESI-MS. The measured rate constants are in agreement with the results of stopped-flow UV−vis spectroscopy and are consistent with those of the steady state kinetic studies. It is demonstrated that time-resolved ESI-MS can serve as a powerful alternative to more established pre-steady state techniques in elucidating enzyme mechanism.

EXPERIMENTAL PROCEDURES

General. The substrate 2,5-dinitrophenyl β-xylobioside (2,5-$DNPX_2$) was synthesized according to published procedures (*51*). The mutation of BCX, yielding the Y80F substitution, has also been described previously (*32*). Prior to kinetic studies, solutions of wild type BCX (MW of 20 400 Da) and mutant BCX Y80F (MW of 20 384 Da) were exhaustively desalted with freshly prepared 10 mM ammonium acetate (pH 6 for wild type and pH 6.30 for the mutant) using a centrifugal concentrator (Amicon) with a nominal molecular mass cutoff of 10 kDa. The concentrations of wild type and mutant BCX were determined from the extinction coefficient $A_{280}^{0.1\%} = 2.50$. This extinction coefficient was derived from active site titration of BCX Y80F with 2,5-$DNPX_2$ (see below).

Steady State Kinetics. Steady state kinetic studies were performed on a Unicam 8700 UV−vis spectrometer equipped with a circulating water bath. Assay solutions, prepared in black quartz curvettes (1 cm path length), consisted of an appropriate concentration of substrate in 5 mM ammonium acetate (pH 6.0 for wild type BCX and pH 6.3 for BCX Y80F), pre-equilibrated at 23 °C. Substrate hydrolysis was initiated with the addition of an aliquot of enzyme (0.629 μg/mL wild type BCX and 220 μg/mL BCX Y80F final concentrations), and the initial rate of phenolate release was monitored at 440 nm ($\Delta\epsilon = 3.57$ mM^{-1} cm^{-1}) (*51*). Hydrolysis rates were determined at 10 substrate concentrations ranging from 0.2 to 5 times the estimated K_m value, where possible. The resulting velocity curve was fitted with the standard Michaelis−Menten equation using the program GraFit (*52*).

Stopped-Flow Spectroscopy. Pre-steady state kinetics were performed on a stopped-flow UV−vis spectrometer (Applied Photophysics, model SF.17MV) equipped with a circulating water bath. Aliquots (100 μL each) of an appropriate concentration of 2,5-$DNPX_2$ (in deionized water) and BCX Y80F (0.41 mg/mL, 20 μM, in 10 mM ammonium acetate at pH 6.3) were pneumatically driven from 2.5 mL Hamilton syringes (equilibrated at 23 °C) into a mixing cell. The release of phenolate was monitored at 440 nm for a total of

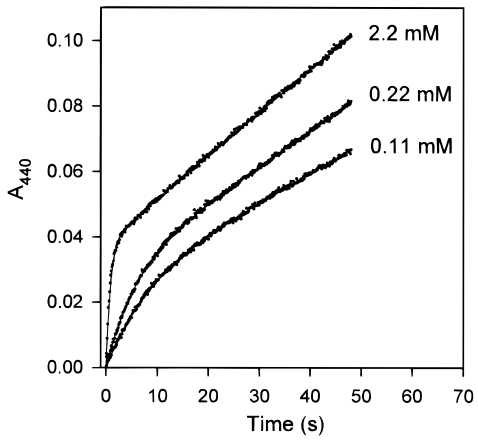

FIGURE 1: Pre-steady state kinetic analysis of the hydrolysis of 2,5-DNPX_2 by BCX Y80F (0.20 mg/mL, 10 μM), monitoring the release of 2,5-DNP by stopped-flow UV−vis spectroscopy. The substrate concentrations for the individual curves are as indicated.

50 s, and the resulting time course was fitted to the equation $A_{440}(t) = A[1 - \exp(-k_{obs}t)] + Bt + C$ using the program GraFit. The observed first-order rate constant (k_{obs}) for the pre-steady state release of phenolate was determined at seven substrate concentrations (ranging from 0.1 to 2.2 mM).

The published extinction coefficient for BCX ($A_{280}^{0.1\%} = 4.08$) (*32*) is an estimate based on the number of tyrosine and tryptophan residues in the protein, rather than an exact value determined from a complete amino acid quantification. A more accurate measure of enzyme concentration can be derived from the stopped-flow experiments because 2,5-DNPX_2 acts as an active site titrant with BCX Y80F due to rate-limiting deglycosylation ($k_{+2} \gg k_{+3}$) (*40*). When a sample of BCX Y80F, diluted 133-fold from the stock solution, was mixed with excess 2,5-DNPX_2 (2.2 mM), a burst of 10.1 μM 2,5-DNP (0.036 absorbance units) was observed (Figure 1). This corresponds to 0.206 mg/mL enzyme or 27.4 mg/mL stock solution concentrations. Time-resolved ESI-MS measurements indicated that >95% of the enzyme is converted to E−X_2 under these conditions (see below); therefore, it is unlikely that this burst underestimates the concentration of enzyme (*40*). A 561-fold dilution of the stock solution yielded an absorbance of 0.122 at 280 nm, which corresponds to an extinction coefficient $A_{280}^{0.1\%}$ of 2.50.

Time-Resolved ESI-MS. Time-resolved ESI-MS measurements were carried out as described previously (*13*, *14*). Briefly, two syringes (1 mL each) were advanced simultaneously by a syringe pump. One syringe contained enzyme (0.165 mg/mL wild type or BCX Y80F) in 10 mM ammonium acetate buffer (pH 6.0 for wild type BCX and pH 6.3 for BCX Y80F). The other syringe contained 2,5-DNPX_2 in deionized water. The enzymatic reaction was initiated by mixing the solutions from both syringes in a reaction tee. This tee was connected to an ESI source by a reaction capillary with an inner diameter of 75 μm. Lengths of the reaction capillaries varied between 1 and 186 cm. The total flow rates used for the experiments were 10 and 20 μL/min, corresponding to minimum and maximum reaction times of 0.13 and 47.8 s, respectively. Slightly different charge state distributions were observed at different flow rates. Therefore, for a given substrate concentration, the flow rate was kept constant and the reaction time was varied only by changing the length of the reaction capillary. Apparently, the velocity distribution in the reaction capillary translates into a narrow distribution of solution "age", even though simple models indicate that the flow rates used might be too low to induce turbulent flow (*41*). This is evident from the excellent agreement between the stopped-flow and time-resolved ESI-MS data in this (see below) and previous studies (*13*, *14*). The enzyme and substrate concentrations given in the remainder of this article correspond to the final concentrations (i.e., after the mixing step). Multiply charged gas phase protein ions were generated at the exit of the reaction capillary by pneumatically assisted ESI and were analyzed in a quadrupole mass spectrometer constructed "in house" (*14*). The voltage difference between the orifice and the RF-only quadrupole ("declustering voltage") was 130 V unless stated otherwise. All experiments were carried out at room temperature (23 ± 1 °C). The relative ratio of E−X_2 to free enzyme at a given time point was determined from the relative intensities (peak heights) of the 8^+ ions, averaged from 30 scans. The time courses for the accumulation of E−X_2 were fit to the equation $C(t) = C_{SS}[1 - \exp(-k_{obs}t)]$, where $C(t)$ is the concentration of E−X_2 as a function of time t and C_{SS} is the steady state concentration of E−X_2. The first-order rate constant, k_{obs}, was determined at eight concentrations of 2,5-DNPX_2 ranging from 0.035 to 2.2 mM.

Pre-Steady State Analysis. According to Scheme 1, the first-order rate constant for the release of phenolate, or the accumulation of E−X_2, is given by (*39*, *47*)

$$k_{obs} = k_{+3} + \frac{k_{+2}[S]}{K_d + [S]} \quad (1)$$

In the absence of saturation kinetics ([S] < K_d), eq 1 simplifies to

$$k_{obs} = k_{+3} + \frac{k_{+2}[S]}{K_d} \quad (2)$$

Pre-steady state kinetic parameters were therefore determined by fitting values of k_{obs} measured at each substrate concentration to these equations using GraFit (*52*).

RESULTS AND DISCUSSION

Steady State Kinetics and Stopped-Flow Spectroscopy. The kinetic behavior of a retaining glycosidase such as BCX may be analyzed with the three-step mechanism illustrated in Scheme 1. To monitor meaningful pre-steady state kinetics for the formation of the covalent intermediate E−X_2, or the corresponding release of 2,5-DNP, the deglycosylation step must be rate-limiting ($k_{+2} > k_{+3}$). In the case of the wild type BCX, glycosylation (k_{+2}) is rate-limiting, even with the most reactive of aryl-β-xylobiosides (*36*, *37*). The corresponding Y80F mutant hydrolyzes 2,5-DNPX_2 480-fold slower ($k_{cat} = 0.042$ s^{-1}) than the wild type enzyme ($k_{cat} = 20$ s^{-1}), while a substantially lower K_m (60 μM for the mutant and 1.8 mM for wild type) suggests the accumulation of E−X_2. That deglycosylation is now rate-limiting is verified by the pre-steady state bursts of 2,5-DNP observed by stopped-flow UV−vis spectroscopy (Figure 1). This change

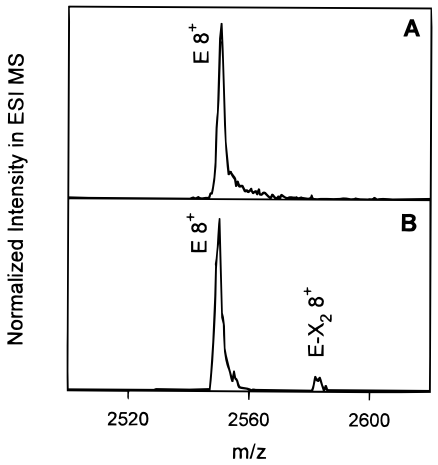

FIGURE 2: Detection of a transient enzyme intermediate with time-resolved ESI-MS. ESI mass spectra of wild type BCX (0.08 mg/mL, 4 μM) recorded before (A) and after mixing with 2,5-DNPX_2 (2.2 mM) for 130 ms (B). Only the 8^+ peaks are shown. The small peak at m/z = 2583 (B) corresponds to the covalent xylobiosyl−enzyme intermediate (E−X_2).

in rate-determining step supports the role of Tyr80 in positioning Glu172 and perturbing its pK_a through a hydrogen bond to the carboxyl group (*32*, *37*). The loss of this interaction in the Y80F mutant has been observed to increase the pK_a's of Glu172 (from 6.8 to 7.8) and Glu78 (from 4.6 to 4.8), resulting in a shift in pH optimum from 5.7 to 6.3 (M. D. Joshi and L. P. McIntosh, unpublished). This substantial increase in pK_a for the general acid−base catalyst can be expected to reduce both glycosylation and deglycosylation rates. However, the reactive aglycone of 2,5-DNPX_2 (pK_a = 5.1) does not require general acid catalytic assistance for departure; therefore, hydrolysis rates will be limited only by the deglycosylation step, resulting in accumulation of E−X_2. It is interesting to note that the Y80F mutation has a greater deleterious effect on the hydrolysis rate of 2,5-DNPX_2 than mutations that eliminate general acid−base catalysis altogether (E172N and E172S) (*37*), underscoring the importance of this residue to catalysis.

Observation of the Covalent Intermediate E−X₂ by Time-Resolved ESI-MS. As noted above, the rate-limiting step for wild type BCX is glycosylation, even with the reactive substrate 2,5-DNPX_2. However, the glycosylation and deglycosylation rates must be on the same order of magnitude because a low steady state concentration (~5%) of E−X_2 was detected in the time-resolved ESI mass spectrum when BCX was mixed with 2.2 mM 2,5-DNPX_2, a concentration which afforded approximately half-saturation of the enzyme (K_m = 1.8 mM) (Figure 2B). If glycosylation had been very much slower than deglycosylation ($k_{+2} \ll k_{+3}$), E−X_2 would not have accumulated to a detectable level. It is noteworthy that indirect detection of E−X_2 had been impossible using stopped-flow UV−vis spectroscopy (*37*); indeed, this intermediate had only been accessible through trapping with a mechanism-based inactivator (*34*).

The ESI mass spectrum of the mutant BCX Y80F in 5 mM ammonium acetate buffer (pH 6.3, no substrate) displayed a charge state distribution that was virtually identical to that of the wild type enzyme, with a characteristic maximum at 8^+ (data not shown). The m/z values of the peaks in the spectrum agreed with the calculated mass of the mutant (MW = 20 384 Da). A very similar spectrum

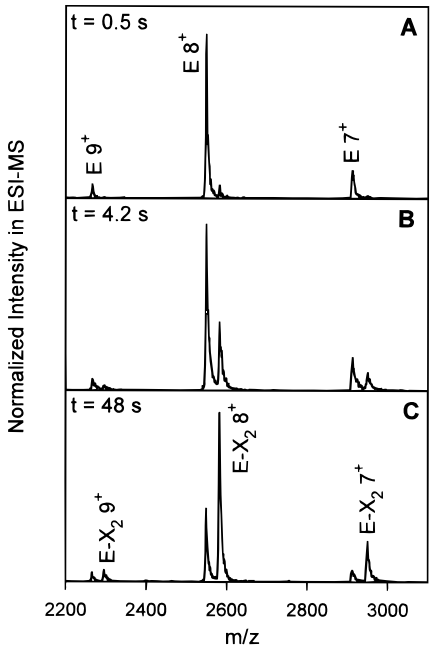

FIGURE 3: ESI mass spectra recorded 0.5 s (A), 4.2 s (B), and 48 s (C) after mixing a solution of BCX Y80F (0.08 mg/mL, 4 μM) with the substrate 2,5-DNPX_2 (110 μM). Peaks in the spectrum correspond to free enzyme (E) and the covalent xylobiosyl−enzyme intermediate (E−X_2).

was recorded 0.5 s after mixing the enzyme with 0.11 mM 2,5-DNPX_2 (Figure 3A). However, after 4.2 s (Figure 3B), each of the peaks in the spectrum displayed a pronounced satellite peak. On the basis of the m/z values, these satellite peaks can be assigned to the covalent xylobiosyl−enzyme intermediate E−X_2 (MW = 20 649 Da). The spectrum recorded after 48 s (Figure 3C) displayed an even higher intensity for the E−X_2 peaks. Similar intensity ratios between E and E−X_2 peaks were observed for the different charge states for all reaction times and substrate concentrations.

Pre-Steady State Kinetic Studies of E−X₂ Formation Monitored by Time-Resolved ESI-MS. From Figure 3, it is evident that the ESI charge state distributions for the free enzyme E and the intermediate E−X_2 are very similar; both have most of their overall intensity in the respective 8^+ peak. The average of several spectra afforded reproducible intensity ratios for the two 8^+ peaks, which can be used as a measure of the relative concentration of E−X_2 in solution as a function of time. Measurement of peak areas gave identical values for the fraction of E−X_2. The results of some representative pre-steady state kinetic measurements are shown in Figure 4. Consistent with the kinetic scenario in which $k_{+2} > k_{+3}$ (Scheme 1), the steady state concentration of the covalent complex E−X_2 with saturating substrate comprised 95% of the total enzyme. As observed for the rate of phenolate release (Figure 1), the pre-steady state accumulation of E−X_2 follows first-order kinetics. The dependence of k_{obs} on substrate concentration is shown in Figure 5. The absence of any saturation behavior indicates that the K_d value for binding of 2,5-DNPX_2 to BCX Y80F is in the high millimolar range, consistent with K_m values measured previously for the hydrolysis of less reactive substrates by wild type BCX (*51*).

Noncovalent Enzyme−Substrate Complex E−DNPX₂. The spectra in Figure 3 do not show any peaks that could be

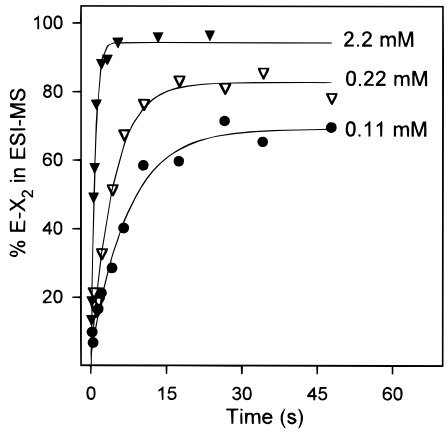

FIGURE 4: Relative contribution of the 8^+ ion generated from the covalent xylobiosyl−enzyme intermediate (E−X_2) in the ESI mass spectrum as a function of time. The substrate concentrations for the individual curves are as indicated. Circular and triangular symbols represent experimental data; solid lines are single-exponential fits to the data.

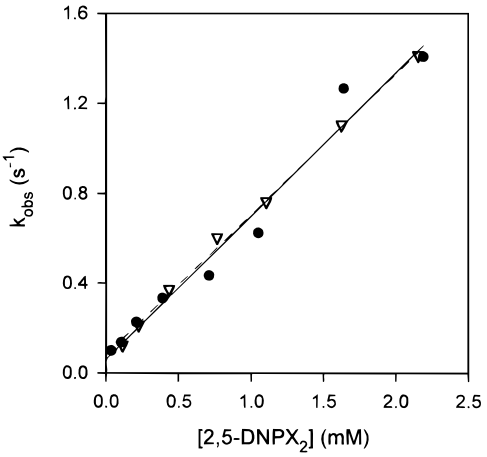

FIGURE 5: Validation of time-resolved ESI-MS by stopped-flow UV−vis spectroscopy. The first-order rate constant (k_{obs}) for the pre-steady state accumulation of E−X_2 (●), monitored by time-resolved ESI-MS, and the corresponding release of 2,5-DNP (▽), monitored by stopped-flow UV−vis spectroscopy, plotted as a function of 2,5-$DNPX_2$ concentration. Linear fits of the data derived from each method are shown as solid and dashed lines.

assigned to noncovalent enzyme−substrate or enzyme−product complexes. Recently, it was observed that noncovalent inhibitor complexes formed by trypsin could only be detected by ESI-MS at low declustering voltages (*54*). Similar attempts were made to detect noncovalent complexes formed by BCX Y80F under very "mild" ion sampling conditions (declustering voltage of 30 V). Under these conditions, a whole series of peaks was observed for each charge state which could be assigned to gas phase ions having the composition E−$(DNPX_2)_n$, with values of n ranging from 0 to about 5. This series is most likely due to the formation of nonspecific gas phase adducts rather than specific enzyme−substrate or enzyme−product complexes. This notion is supported by the observation of similar clusters for the covalent intermediate E−X_2 [i.e., E−$X_2(DNPX_2)_n$] under saturating steady state conditions. That specific enzyme−substrate complexes are not observed in this system is not surprising; Ganem et al. have shown previously with hen egg white lysozyme that specific noncovalent complexes are only observed when the dissociation constant is in the micromolar range or lower (*17*). As noted above, the K_d values in this case are much higher.

Stopped-Flow UV−Vis Spectroscopy Compared to Time-Resolved ESI-MS. As dictated by the kinetic mechanism shown in Scheme 1, the first-order rate of release of 2,5-DNP in the pre-steady state must be equal to the rate of accumulation of E−X_2. On this basis, traditional stopped-flow UV−vis spectroscopy can be used to verify the accuracy of time-resolved ESI-MS. The linear fits of the data in Figure 5 (solid and dashed lines) show that the correlations of k_{obs} with substrate concentration determined by each method agree very well, within experimental error. The low solubility of 2,5-$DNPX_2$ precluded saturation of BCX Y80F in the pre-steady state; therefore, eq 1 could not be used to determine the individual values for k_2 and K_d. However, according to eq 2, the slope of the plots in Figure 5 yields a value for the second-order rate constant k_2/K_d of 0.65 mM^{-1} s^{-1}. This is in excellent agreement with the corresponding value for the second-order rate constant k_{cat}/K_m of 0.70 mM^{-1} s^{-1}, obtained from the steady state kinetics.

CONCLUSIONS

This study demonstrates that the pre-steady state kinetic parameters for the hydrolysis of 2,5-$DNPX_2$ by BCX Y80F can be determined by time-resolved ESI-MS. Identical kinetic parameters are obtained using traditional stopped-flow UV−vis spectroscopy, thereby verifying the accuracy of this new technique. The time resolution of the apparatus used in this work is currently limited to tens of milliseconds (*13*), this being determined by the length of the reaction capillary, and is therefore limited to enzymes with k_{cat} values less than ~10 s^{-1}. Rapid chemical quench methods for monitoring enzyme intermediates currently can provide better time resolution. However, these methods require the use of radiolabeled substrates and are prone to artifacts arising from nonspecific entrapment of the radioactive label. This is not a problem with the time-resolved ESI-MS technique. As well, considerable improvements in flow rate are possible. Indeed, the pulsed-flow apparatus used by Paiva et al. (*26*) for time-resolved ESI-MS generated flow rates approximately 100-fold larger than those used in this study. As noted by Northrop and Simpson (*15*), the advantage of time-resolved ESI-MS over traditional pre-steady state techniques is the unambiguous identification of mechanistically important intermediates by direct observation of their mass. This advantage was aptly demonstrated by ESI-MS studies on the inhibition of TEM-2 β-lactamase by clavulanic acid, in which the observed mass of the acyl−enzyme intermediate formed was 44 Da less than predicted, the result of decarboxylation of the inhibitor following acylation of the enzyme (*21*, *22*). As well, time-resolved ESI-MS does not require chromophoric substrates, thereby providing an opportunity to conduct enzyme kinetics with more "native" substrates without the need for coupled assays (*15*). Moreover, in principle, it is possible to simultaneously observe product formation and substrate depletion in addition to monitoring the formation and depletion of enzyme intermediates. Therefore, a host of kinetic data may be generated in a single experiment. These wider applications of time-resolved ESI-MS will be the focus of future research.

ACKNOWLEDGMENT

In addition to helpful discussions, we are indebted to Manish Joshi and Lawrence McIntosh for generous gifts of wild type BCX and the Y80F mutant.

REFERENCES

1. Fenn, J. B., Mann, M., Meng, C. K., et al. (1989) *Science 246*, 64−71.
2. Mann, M., and Wilm, M. (1995) *Trends Biochem. Sci. 20*, 219−224.
3. Loo, J. A. (1997) *Mass Spectrom. Rev. 16*, 1−23.
4. Chowdhury, S. K., Katta, V., and Chait, B. T. (1990) *J. Am. Chem. Soc. 112*, 9012−9013.
5. Miranker, A., Robinson, C. V., Radford, S. E., et al. (1993) *Science 262*, 896−900.
6. Konermann, L., and Douglas, D. J. (1997) *Biochemistry 36*, 12296−12302.
7. Konermann, L. (1998) *Sci. Prog. 81* (in press).
8. Wood, T. D., Chorush, R. A., Wampler, F. M., et al. (1995) *Proc. Natl. Acad. Sci. U.S.A. 92*, 2451−2454.
9. Clemmer, D. E., Hudgins, R. R., and Jarrold, M. F. (1995) *J. Am. Chem. Soc. 117*, 10141−10142.
10. Collings, B. A., and Douglas, D. J. (1996) *J. Am. Chem. Soc. 118*, 4488−4489.
11. Loo, J. A. (1995) *Bioconjugate Chem. 6*, 644−665.
12. Przybylski, M., and Glocker, M. O. (1996) *Angew. Chem., Int. Ed. Engl. 35*, 806−826.
13. Konermann, L., Rosell, F. I., Mauk, A. G., et al. (1997) *Biochemistry 36*, 6448−6454.
14. Konermann, L., Collings, B. A., and Douglas, D. J. (1997) *Biochemistry 36*, 5554−5559.
15. Northrop, D. B., and Simpson, F. B. (1997) *Bioorg. Med. Chem. 5*, 641−644.
16. Cheng, X., Chen, R., Bruce, J. E., et al. (1995) *J. Am. Chem. Soc. 117*, 8859−8860.
17. Ganem, B., Li, Y.-T., and Henion, J. D. (1991) *J. Am. Chem. Soc. 113*, 7818−7819.
18. Ashton, D. S., Beddell, C. R., Cooper, D. J., et al. (1991) *FEBS Lett. 292*, 201−204.
19. Knight, W. B., Swiderek, K. M., Sakuma, T., et al. (1993) *Biochemistry 32*, 2031−2035.
20. Aplin, R. T., Baldwin, J. E., Schofield, C. J., et al. (1990) *FEBS Lett. 277*, 212−214.
21. Brown, R. P., Aplin, R. T., and Schofield, C. J. (1996) *Biochemistry 35*, 12421−12432.
22. Brown, R. P., Aplin, R. T., Schofield, C. J., et al. (1997) *J. Antibiot. (Tokyo) 50*, 184−185.
23. Tull, D., Miao, S., Withers, S. G., et al. (1995) *Anal. Biochem. 224*, 509−514.
24. McCarter, J. D., and Withers, S. G. (1996) *J. Am. Chem. Soc. 118*, 241−242.
25. Lee, E. D., Muck, W., Henion, J. D., et al. (1989) *J. Am. Chem. Soc. 111*, 4600−4604.
26. Paiva, A. A., Tilton, R. F., Crooks, G. P., et al. (1997) *Biochemistry 36*, 15472−15476.
27. Northrop, D. B., and Simpson, F. B. (1997) *FASEB J. 11*, A1021.
28. Henrissat, B. (1991) *Biochem. J. 280*, 309−316.
29. Gebler, J., Gilkes, N. R., Claeyssens, M., et al. (1992) *J. Biol. Chem. 267*, 12559−12561.
30. Koshland, D. E. (1953) *Biol. Rev. 28*, 416−436.
31. Sinnott, M. L. (1990) *Chem. Rev. 90*, 1171−1202.
32. Wakarchuk, W. W., Campbell, R. L., Sung, W. L., et al. (1994) *Protein Sci. 3*, 467−475.
33. Plesniak, L. A., Wakarchuk, W. W., and Mcintosh, L. P. (1996) *Protein Sci. 5*, 1118−1135.
34. Miao, S., Ziser, L., Aebersold, R., et al. (1994) *Biochemistry 33*, 7027−7032.
35. Withers, S. G., and Aebersold, R. (1995) *Protein Sci. 4*, 361−372.
36. Lawson, S. L., Wakarchuk, W. W., and Withers, S. G. (1996) *Biochemistry 35*, 10110−10118.
37. Lawson, S. L., Wakarchuk, W. W., and Withers, S. G. (1997) *Biochemistry 36*, 2257−2265.
38. McIntosh, L. P., Hand, G., Johnson, P. E., et al. (1996) *Biochemistry 35*, 9958−9966.
39. Hiromi, K. (1979) *Kinetics of Fast Enzyme Reactions*, John Wiley & Sons, New York.
40. Fersht, A. (1985) *Enzyme Structure and Mechanism*, 2nd ed., W. H. Freeman & Co., New York.
41. Johnson, K. A. (1995) *Methods Enzymol. 249*, 38−61.
42. Fierke, C. A., and Hammes, G. G. (1995) *Methods Enzymol. 249*, 3−37.
43. Tull, D., and Withers, S. G. (1994) *Biochemistry 33*, 6363−6370.
44. MacLeod, A. M., Tull, D., Rupitz, K., et al. (1996) *Biochemistry 35*, 13165−13172.
45. Gebler, J. C., Trimbur, D. E., Warren, R. A. J., et al. (1995) *Biochemistry 34*, 14547−14553.
46. Wang, Q., Trimbur, D., Graham, R., et al. (1995) *Biochemistry 34*, 14554−14562.
47. Namchuk, M. N., and Withers, S. G. (1995) *Biochemistry 34*, 16194−16202.
48. Fink, A. L., and Angelides, K. J. (1975) *Biochem. Biophys. Res. Commun. 64*, 701−708.
49. Withers, S. G. (1977) Ph.D. Thesis, Department of Chemistry, University of Bristol, Bristol, U.K.
50. Deschavanne, P. J., Viratelle, O. M., and Yon, J. M. (1978) *Proc. Natl. Acad. Sci. U.S.A. 75*, 1892−1896.
51. Ziser, L., Setyawati, I., and Withers, S. G. (1995) *Carbohydr. Res. 274*, 137−153.
52. Leatherbarrow, R. J. (1994) *GraFit*, Erithacus Software, Ltd., London.
53. Kraunsoe, J. A., Aplin, R. T., Green, B., et al. (1996) *FEBS Lett. 396*, 108−112.

BI980445O